Electrostatic properties of maghemite (γ- $Fe_2O_3$) nanocrystalline quantum dots determined by electrophoretic deposition



2009 J. Phys.: Condens. Matter 21 285301

(http://iopscience.iop.org/0953-8984/21/28/285301)

J. Phys.: Condens. Matter **21** (2009) 285301 (8pp) doi:10.1088/0953-8984/21/28/285301

# Electrostatic properties of maghemite ($\gamma$-$Fe_2O_3$) nanocrystalline quantum dots determined by electrophoretic deposition

**Mohammad A Islam**[1,2] **and Shengguo Xia**[2]

[1] Department of Physics, American University of Sharjah, Sharjah, United Arab Emirates
[2] Columbia Center for Nanostructured Materials, Columbia University, New York, NY, USA

E-mail: mislam@aus.edu

Received 20 January 2009, in final form 25 May 2009
Published 17 June 2009
Online at stacks.iop.org/JPhysCM/21/285301

**Abstract**

We applied a DC electric field between two flat electrodes to attract thermally charged maghemite ($\gamma$-$Fe_2O_3$) nanocrystalline quantum dots dissolved in hexane to form smooth, robust, large area and apparently identical films of equal thickness on both electrodes. Visible microscopy, scanning electron microscopy, atomic force microscopy and profilometry showed that the electrophoretically deposited dot films were very smooth with an rms roughness of $\sim$10 nm for $\sim$0.2 $\mu$m thick films. The films were of high quality. They did not re-dissolve in hexane (as do those formed by dry casting), which is a good solvent for these dots, or in common cleaning solvents such as water, alcohols and acetone. The deposition on both electrodes implies there are both positively and negatively thermally charged dots, unlike conventional electrophoretic deposition. We used simple thermodynamics to explain the results of electrophoretic deposition macroscopically. To connect the macroscopic nature of the deposition to the microscopic nature of the dots we performed electrophoretic mobility measurements of the dots and the results seem to complement the thermodynamic treatment.

(Some figures in this article are in colour only in the electronic version)

## 1. Introduction

Iron oxides are ubiquitous in nature and play important roles in a variety of disciplines, including environmental and industrial chemistry, corrosion science, geology, biology, soil science, medicine and so on. They are of great significance for many biological and ecological systems. Maghemite ($\gamma$-$Fe_2O_3$) is one of the most important iron oxides in the environment since it is found in abundant quantities in the soils of the tropics and the subtropics [1]. The iron oxides found freely in nature are of poor crystal quality. In most cases the crystals are less than 100 nm in size and have defects and impurities. Because of the nanocrystalline nature of natural iron oxides they have a very high surface to volume ratio and the surface chemistry plays major roles in the properties of these oxides [1]. Therefore, nanocrystalline quantum dots (NQDs) of maghemite with sizes in the range of 2–12 nm give us the opportunity to understand and investigate the properties of iron oxides found in nature. The abundance of surface states in the NQDs, some of which are passivated by ligands like oleic acid and some of which remain dangling, presents theorists and experimentalists with challenges and opportunities for surface engineering [2]. The formation of arrays of maghemite NQDs is important for understanding and exploring their collective behavior, something very similar to what might happen in real soil chemistry. At the present time films of NQDs are mostly formed by dry casting or spin coating. Semiconductor [3], metal [4–6] and magnetic NQDs [7, 8] have been self-assembled to make quantum dot superlattices by conventional methods of dry casting and spin coating. Films formed by these methods are not very uniform and thickness control is somewhat coarse. In this paper we report the electrophoretic deposition (EPD) of maghemite NQDs with diameters in the range of 3.4–12 nm on Au-on-Si electrodes. The resulting films are smooth and robust. Our EPD method [9] is an extremely simple one, and yet provides us with an enormous amount of insight into the electrostatics of the maghemite dots. We show that a fraction of the dots

 

are thermally charged and the percentage of the charged dots depends on the dot diameter. We used simple thermodynamics to explain the different percentages of charged dots. To connect the macroscopic nature of the deposition to the microscopic nature of the dots we performed electrophoretic mobility measurements for the dots and the results seem to complement the thermodynamic treatment. The electrophoretic mobility measurements show that there is an asymmetry in the charging of the dots, providing us with opportunity to fabricate NQD heterostructures.

## 2. Experimental procedures

Colloidal maghemite NQDs were prepared according to the method of Hyeon *et al* [8]. Briefly, trioctylamine and oleic acid were heated and degassed. Iron pentacarbonyl was injected into this mixture and the mixture was heated. The change of color of the mixture from yellow to black indicates the formation of Fe NQDs. Maghemite NQDs are formed when the Fe NQDs are oxidized using a suitable oxidizer; we used trimethylamine-*n*-oxide dihydrate dissolved in toluene. All the chemicals were purchased from Aldrich Chemicals, USA. The exact amount of reagents used for a typical synthesis run is given in [8].

When the dots are synthesized initially their size is found to be around 2.8 nm. Continuous heating while oxidizing results in an increase in the size of the dots. For the purpose of this paper, we synthesized maghemite dots of sizes 3.4, 4.2, 5.2 and 12 nm.

Solutions of these dots were made in hexane solvent with densities between $1 \times 10^{12}$ and $1 \times 10^{13}$ dots cm$^{-3}$, which corresponds to volume fractions of $1.0 \times 10^{-6}$%–$1.2 \times 10^{-5}$% for 12 nm diameter dots. Au-on-Si electrodes were prepared by depositing ∼10 nm Ti and then ∼150 nm Au on 0.8 cm × 1.4 cm rectangular sections of Si(100) wafers covered with an approximately 1 $\mu$m thick thermal $SiO_2$. A pair of these electrodes was separated by ∼2.0 mm and was submerged in a beaker with the dot solution. DC voltages up to 1000 V were applied across the electrodes at room temperature in the dark, with solvent added as needed to counter any solvent evaporation, since hexane is an extremely volatile solvent.

DC current was monitored during the deposition, and the films on the electrodes were examined afterwards using visible microscopy, scanning electron microscopy (SEM), atomic force microscopy (AFM) and profilometry.

Electrophoretic mobility measurements [10] of the maghemite NQDs in hexane were performed before and after the EPD experiments by using a Malvern Zetasizer Nano instrument, with irradiation from a 4 mW 632.8 nm He–Ne laser. The samples were filled in dip cells, fitted with Pt electrodes with a pair of electrodes separated by 2.0 mm. An alternating square voltage was applied during the measurements (with a nominal voltage of 40 V) [11, 12]. Each presented plot in figure 5 represents an average of four measurements, and each measurement consists of 200 repetitions of a 2 s long scan. All data were collected at 25 °C. The combination of laser Doppler velocimetry and phase analysis light scattering (PALS) allows the determination of the entire electrophoretic mobility distribution for a given species instead of only an average mobility [11, 12].

## 3. Measurements and results

For 12 nm diameter maghemite dots the initial current density between the electrodes was ∼6.8 nA cm$^{-2}$ for 530 V ($2.5 \times 10^5$ V m$^{-1}$), and $4.0 \times 10^{12}$ dots cm$^{-3}$, and it decreased to ∼0.61 nA cm$^{-2}$ in 30 min as shown in figure 1(a). The current density was linearly proportional to the voltage $V$ when the particle density $n$ was kept constant, and it was linearly proportional to the particle density $n$ when the voltage $V$ when was kept constant. These plots were found to be straight lines with almost zero intercepts and are not shown. Without the dots the current was ∼40× smaller with the hexane solvent only.

After long runs (12 nm diameter dots, 30 min, 530 V, $4.0 \times 10^{12}$ dots cm$^{-3}$) 180 nm thick, apparently identical, films were deposited on both electrodes. No deposit was formed without the voltage. Visible microscopy, SEM, profilometry and AFM showed that both films were smooth, with ∼10 nm rms roughness for the 0.18 $\mu$m thick film, as shown in figures 1(b)–(d). To get a consistent estimate of the quality and roughness of the films we performed three line scans and the results are shown in figure 1(c). The film thickness was determined by scratching off part of the film and performing an AFM scan.

To ensure that the deposits on the electrodes were indeed films of maghemite dots, we performed EPD of the dot solution on ITO coated glass electrodes (transparent) and compared the absorbance (transmission) spectrum of these transparent films with that of the original maghemite NQD solution. The spectra were almost identical. These results are not shown for the sake of brevity. Furthermore, we compared the XPS spectra of a dry sample of the original maghemite dots with that of the EPD dot films. These spectra were also very close to each other, as shown in figure 2. These results clearly indicate that the films were indeed composed of maghemite NQDs and the EPD does not alter the properties of the dots significantly.

The EPD films were robust. After drying, these films did not re-dissolve in hexane (as do those formed by dry casting), even when a voltage of either polarity was applied across it to a bare Au electrode. The films also did not re-dissolve in common cleaners such as water, methanol, ethanol and acetone.

The initial conductivity of the 12 nm maghemite dot/hexane solution was measured to be $\sigma = 2.57 \times 10^{-10}$ ohm$^{-1}$ m$^{-1}$, since the current density $J$ and electric field $E$ were known. The conductivity of a solution of charged spheres of density $n_c$ in a solvent of viscosity $\eta$ can be calculated using the Einstein–Nernst equation:

$$\sigma = n_c e^2 / 6\pi\eta R, \tag{1}$$

where $R$ is the hydrodynamic radius and $e$ is the charge of each sphere.

In our system, if there are positive and negative dots with densities $n_{c+}$ and $n_{c-}$, then $n_c = n_{c+} + n_{c-}$. Then the equal film thickness on both electrodes suggests $n_{c+} = n_{c-} = n_c/2$,

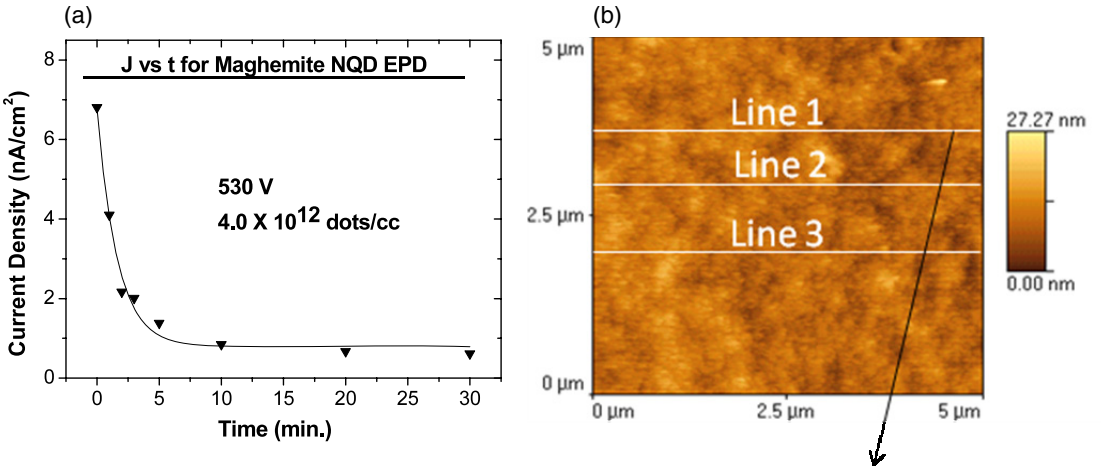


| (c) | Rp-v | Rms Rough |
|---|---|---|
| Line 1 | 20.82 nm | 11.208 nm |
| Line 2 | 25.24 nm | 9.440 nm |
| Line 3 | 22.94 nm | 10.294 nm |

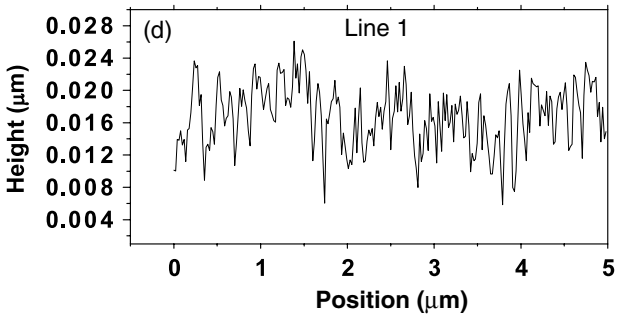


**Figure 1.** (a) The $J$ versus $t$ plot for the EPD of 12 nm diameter maghemite NQDs in hexane solution. (b) AFM image of a 180 nm thick dot film deposited on the negative electrode. (c) A summary of three AFM line scans performed on the EPD film randomly, showing a rms roughness of about 10 nm. (d) Topography of line 1. The results for the films deposited on the positive electrode were very similar and are not shown.

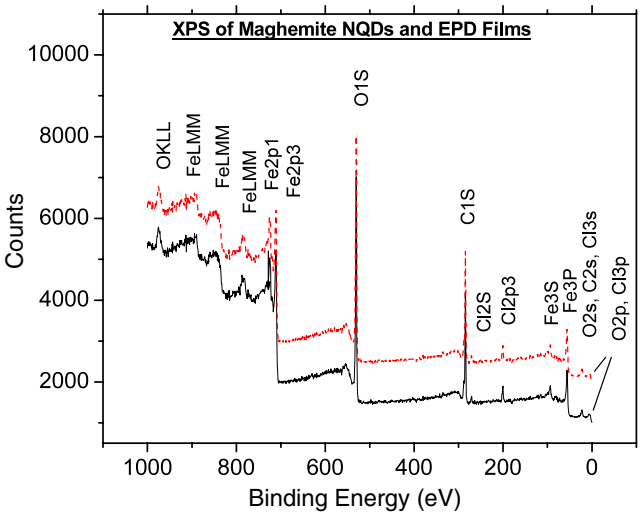


**Figure 2.** XPS of dry maghemite NQD powder (upper plot) and that of EPD film of maghemite NQDs (lower plot). The plots have been intentionally shifted for better viewing.

assuming there are no counter ions. Considering $e$ as the elementary charge, we find $n_c = 4.04 \times 10^{11}$ cm$^{-3}$. When $n_c$ is compared with the initial density of the dots ($4.0 \times 10^{12}$ dots cm$^{-3}$) we found that 10.2% of the dots are charged, half positively and half negatively. Here we are assuming that the dots are simply not large enough to accommodate more than one free charge per dot, a very reasonable assumption as described later in section 4.1. Similar measurements were performed on dots of diameter 3.4 nm, 4.2 nm and 5.2 nm and the results are shown in figure 3(a).

The number of dots deposited was approximated as

$$N_{\text{dep}} = 0.74At/(4\pi R^3/3), \tag{2}$$

where $A$ is the total electrode area, $t$ is the film thickness (the same for each electrode), $R$ is the effective radius of each dot including the capping ligand (6.55 nm for 12 nm diameter dots with an ∼1.1 nm long oleic acid cap) and the 0.74 assumes fcc packing.

The total number of elementary charges collected was calculated by integrating the $I$ versus $t$ plot of figure 1(a) and this was compared to the number of dots deposited. It was found that for the 12 nm diameter maghemite dots, for each elementary charge collected, ∼1.8 dots were deposited. Similar results were found for other dots (figure 4). This could be due to several factors which are discussed later.

Figure 5(a) shows the $\zeta$ potential distribution for the 12 nm diameter maghemite NQDs before and after EPD for a typical run. It shows that the $\zeta$ potential of the dot solution before deposition is significantly asymmetric, with an average value

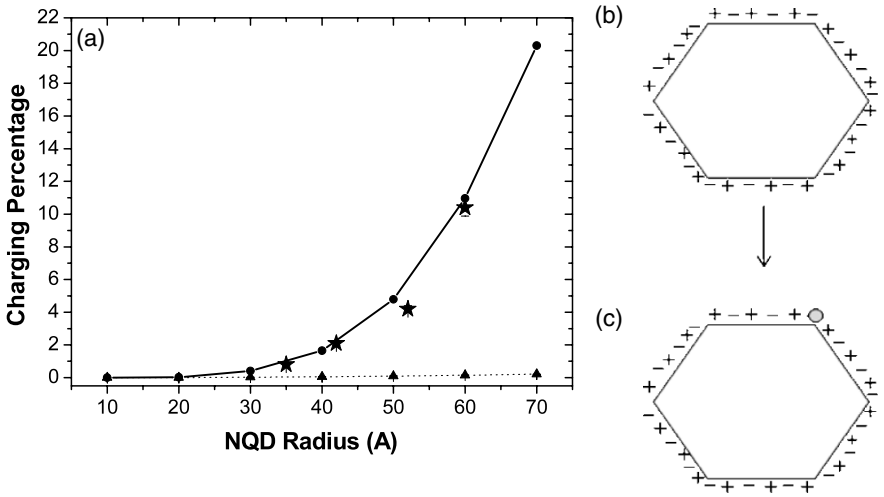


**Figure 3.** (a) ★, experimentally determined percentage of charged maghemite dots in thermal equilibrium. ▲, theoretical charging percentage using $g = 1$ in equation (4). ●, theoretical charging percentage using $g = \alpha \times$ dot surface area, where $\alpha = 6.4 \times 10^{-3}$, in equation (4). (b) Schematic diagram showing the model of faceted maghemite dots with each facet containing a layer of charges on the dot surface. (c) The same maghemite dot with a single negative charge missing; hence it is positively charged. Needless to say, even though for convenience we have shown the dots having six even facets, according to our calculations the number of facets in a 12 nm diameter maghemite dot is around 70 and these facets could come in any shape possible.

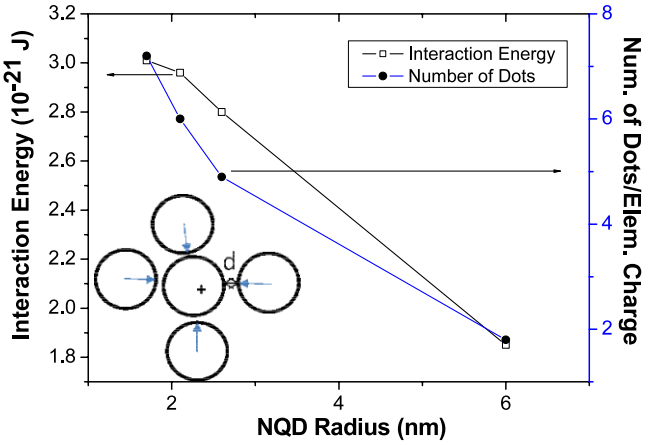


**Figure 4.** The left $y$ axis: dipolar interaction energy between a charged dot and a nearby uncharged dipolar dot as a function of dot radius. The right $y$ axis: number of dots deposited per elementary charge collected, also as function of dot radius. The inset at the lower left corner shows the accumulation of dipolar maghemite dots around a charged dot.

of 18.46 mV, a peak FWHM of 38.4 mV and *a negative fraction of* 18%. After EPD proceeded to form films of the maximum thickness possible (166 nm in this case), there was a dramatic change in the $\zeta$ potential distribution, with the peak shifting towards more positive values, the profile becoming much narrower and the negative fraction almost disappearing. The peak position and the FWHM were 27.8 mV and 23.6 mV, respectively, and the *negative fraction was only* 0.4%.

Immediately after the dc current reached a constant value (figure 1(a)) and the negative fraction in the $\zeta$ potential distribution reached zero (figure 5(a)), we performed a fresh EPD run using a new pair of electrodes in this dot solution. A thin layer of maghemite dot (26 nm) film was deposited in 10 min on the negative electrode as determined by visual observation, AFM scan and XPS spectra. No perceptible deposit was formed on the positive electrode.

The solution in this run was kept in a closed vial to prevent solvent evaporation for 2 days and the $\zeta$ potential re-measured. The results (figure 5(a)) showed that the $\zeta$ potential peak again shifted to lower values and the negative fraction increased. The peak position, the FWHM and the negative fraction were 17.7 mV, 45.0 mV and 23.5%, respectively. Some of this solution was used in a new electrophoretic deposition run using new electrodes and films of approximate thickness 74 nm were deposited on both electrodes in a typical 30 min run.

## 4. Discussions

### *4.1. Thermal charging of maghemite NQDs*

A large fraction of the overall number of atoms in a NQD is on the dot surface, and as such the surface properties play crucial roles in determining many of their important characteristics. The atoms on the dot surfaces create surface dangling bonds which are easily ionizable and can trap free charges from the dot solution; either way we end up with a charged dot.

Because of the abundance of surface states, thermal charging in these states seems to be a strong possibility for the origin of the free charges in the maghemite NQDs. Simple electrostatic considerations can explain this observed charging. Following the work of Brus [13], we can imagine a situation where a dielectric sphere is singly charged and the charging energy is

$$E_C = \sum_{l=0}^{\infty} \frac{e^2(\varepsilon - 1)(l+1)}{2\varepsilon_2(\varepsilon l + l + 1)R} \left(\frac{r}{R}\right)^{2l} \qquad (3)$$

where $\varepsilon = \varepsilon_2/\varepsilon_1$, $\varepsilon_2$ and $\varepsilon_1$ are the dielectric constants of the sphere and the external medium, respectively, $R$ is the radius

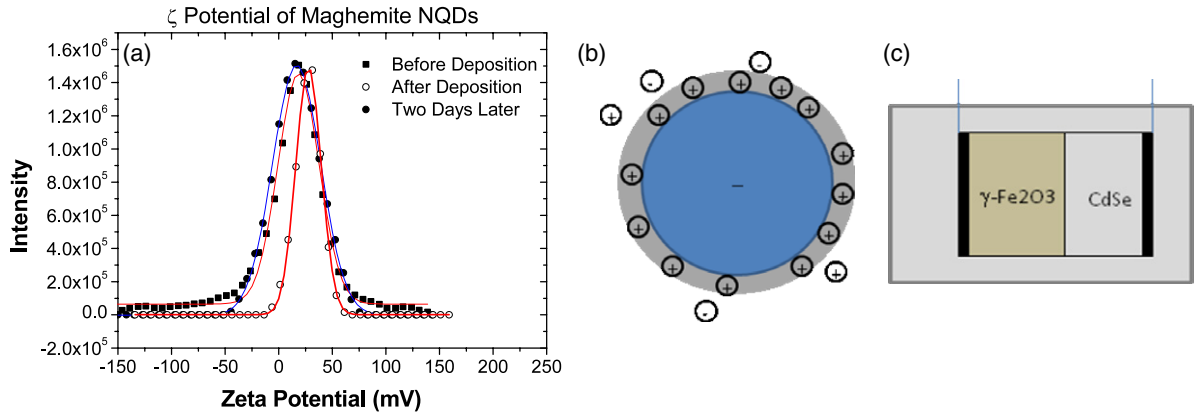


**Figure 5.** (a) $\zeta$ potential distributions of 12 nm diameter maghemite dots in hexane solution at various conditions as described in the plot. (b) The accumulation of positive ions around a negatively charged dot. The dark gray circle is the dot and the light gray shell is the Stern layer. (c) Fabrication of a maghemite dot/CdSe dot heterostructure by exploiting the $\zeta$ potential evolution.

of the dielectric sphere and $r$ is the distance to the free charge inside the dielectric sphere. We consider the dielectric sphere to be composed of a $\gamma$-$Fe_2O_3$ core and, as such, for a 12 nm diameter maghemite dot $R = 6$ nm. We assume the dielectric constant $\varepsilon_2$ of this dielectric sphere to be that of bulk $\gamma$-$Fe_2O_3$, 10.2 [10]. For the outside medium of hexane we take $\varepsilon_1 = 1.8$.

In the absence of extensive theoretical work on maghemite dots, we assume a situation similar to the semiempirical tight binding studies of CdSe NQDs that have shown that the most abundant charged states that lie within the band gap of the core semiconductor are the Se dangling bonds [14]. In the case of the maghemite dots we assume that the free charges are located in the Fe–O dangling bonds *below* the surface of the dots. By taking $r$ to be $R$ minus the Fe–O ionic bond radius of 2.0 Å, $E_c$ can be calculated numerically. For the 12 nm diameter maghemite dots this charging energy is found to be 0.168 eV. Incidentally, if we use $r = R$ or $r > R$, the infinite sum in equation (3) diverges. Theoretical consideration restricts us only to a situation where the free charge can be located at a position inside the dot, i.e. $r < R$.

Boltzmann statistics can be used to explain the results observed in our experiments. Our model is the following: we consider a two-state system where the ground state is a neutral dot and the excited state at $E_c$ above the ground state is the charged dot. Now, we can use Boltzmann statistics to calculate the probability of a dot being charged in thermal equilibrium [15]. For an ensemble of identical NQDs this *probability* should be approximately equal to the *percentage* of charged dots in thermal equilibrium.

For this two-state system where the excited state is degenerate, the probability of the excited state being populated is

$$P(E_c) = \frac{g \exp(-E_c/kT)}{1 + g \exp(-E_c/kT)} \tag{4}$$

where $g$ is the degeneracy ratio.

If we consider a nondegenerate excited state ($g = 1$) our model does not describe the experimental results very well, as shown in figure 3(a). However, if a degeneracy value ($g$) proportional to the dot surface area is used in equation (4) we get a much better correspondence between the experimental results and the model. A reasonably good fit is observed for a surface area $g = \alpha \times$ dot, where $\alpha = 6.4 \times 10^{-3}$ for these maghemite dots (figure 3(a)). For 12 nm diameter maghemite dots this means that the number of Fe–O dangling bonds on the dot surface that are equally capable of trapping the free charges is of the order of 70–80, which is no more than 2% of the total number of atoms on the dot surface; we consider this to be very reasonable [16].

Experiments were carried out with maghemite dots of 3.4, 4.2 and 5.2 nm diameter and similar analyses were performed. The results are shown in figure 3(a).

Similar to what have been seen in CdSe NQDs, we assume that well developed facets in the maghemite NQDs could give rise to the observed charging and the degeneracy of the charged states in these dots [17]. We imagine that the maghemite NQDs possess shape asymmetry of the order of a monolayer and suggest that the charges in this extra monolayer are not as strongly bound to the rest of the NQD as the other internal layers, and are prone to be easily ionizable, giving rise to charged dot, as shown schematically in figures 3(b) and (c). Given the size range (3–12 nm) of the maghemite NQDs we are dealing with, the facets composed of the extra monolayer of charges cannot be so large as to accommodate more than one free charge. Even though the TEM images do not show exact three-dimensional images of the spherical NQDs, our results seem to indicate that the number of facets with an extra monolayer of charges in the maghemite NQDs in the size range of 3–12 nm should be a few tens; we consider this to be a very reasonable number.

This thermodynamic treatment of charging in the maghemite NQDs does not differentiate between the electrons and holes, and as a result the probability of a maghemite NQD of any kind being positively charged or negatively charged should be equal. This is consistent with the results of our EPD experiments: we saw identical film formation on both the anode and the cathode.

Furthermore, our experiments show that the number of dots deposited is much more than the number of initially charged dots. This is also consistent with thermal charging of the dots. Once the charged dots are depleted from the hexane

solution due to deposition on the electrodes, the remaining uncharged dots in the solution get thermally charged, and the deposition/regeneration cycle continues.

### *4.2. Transport of uncharged maghemite dots with dipole moments*

As seen in figure 3, and as discussed in section 3, only a few per cent of the maghemite dots are charged and the number of dots deposited is much higher than the number of elementary charges collected. For example, for 12 nm diameter dots ∼10.9% of the dots are charged, and for each elementary charge collected about 1.8 dots are deposited; for 4.2 nm diameter dots ∼2.1% of the dots are charged and for each elementary charge collected about six dots are deposited. This indicates that uncharged dots are collected on the electrodes along with the charged dots.

We attempt to explain this in the following way: dots with dipole moments are attracted to the charged dots and carried along with them. The dipole moments can be induced in the uncharged dots by a nearby charged dot. Dipolar dots accumulate around the charged dots and as long as this accumulation energy is larger than a *fraction* of the thermal agitation ($kT$) the accumulation will continue. Beyond a certain distance from the charged dot, the accumulation energy will be overcome by the thermal energy and the accumulation will stop. Accordingly, each charged dot will carry a certain number of uncharged dipolar dots with it on its way to the electrode.

The dipole induced in a polarizable medium (e.g. NQDs) by an electric field $E$ is given by [18, 19]

$$\mu = \tfrac{1}{2}\pi\varepsilon_0\varepsilon_1 a^3 \kappa E \tag{5}$$

where $\varepsilon_1$ is the dielectric constant of the fluid, $a$ is the diameter of the dot and $\kappa = (\varepsilon_2 - \varepsilon_1)/(2\varepsilon_1 + \varepsilon_2)$, where $\varepsilon_2$ is the dielectric constant of the dots. The energy ($U$) of a polarized dot with dipole moment given by equation (5) in the electric field of the a nearby charged dot can be calculated using $U = \mu E$, where $E = 1/(4\pi\varepsilon_0)(e/(a+d)^2)$ is the electric field at the center of the induced dipole due to the presence of the nearby charged dot and $d$ is the distance between the dots as shown in the lower left inset to figure 4. When the expression of the induced dipole $\mu$ is substituted into $U$, the energy is found to be equal to

$$U = l \times r^3/(a+d)^4, \tag{6}$$

where $l = \varepsilon_1\kappa e^2/(4\pi\varepsilon_0)$ and $r$ is the radius of the dots. The results for the interaction energy are shown in figure 4.

Even though, compared to $kT = 4.14 \times 10^{-21}$ J, these numbers are a bit smaller, the trends are nonetheless similar to the experimental results: smaller dots have high dipolar energy which leads to higher accumulation around these dots. Also, as discussed earlier in this section, only a fraction of the $kT$ will disrupt the dipolar accumulation because of its random nature. Furthermore, in addition to the dipole moments, quadrupole moments will be induced in the uncharged NQDs by the electric field of the charged dot; this will also enhance dipolar accumulation.

### *4.3. Charge asymmetry in maghemite NQDs*

As described in section 3, we found equal film deposition on the positive and the negative electrodes. In section 4.1 we performed a macroscopic analysis of the results using simple thermodynamics and concluded that in the hexane solution there are equal numbers of positively and negatively charged maghemite dots. A closer look using electrophoretic mobility measurements, however, paints a somewhat different and yet complementary picture.

Before venturing to discuss the results of the electrophoretic mobility measurements, it might be instructive to take a brief look at the nature of the interaction between a charged colloidal particle and the solvent it is dissolved in. When particles and ions coexist in a system, they carry equal and opposite charges to maintain charge balance. The interfacial region including these two charged parts is called the 'electrical double layer' [20]. Let us assume that we have a negatively charged colloidal particle dissolved in a nonaqueous solvent (e.g. maghemite NQDs in hexane). Even though the solvent is nonaqueous, there might still be ions in the solution which could come from the colloidal synthesis of the dots and free capping molecules in the solution. When an electric field $E$ is applied to the solution, the stationary velocity of the particle can be derived by equating the Coulomb force ($F_{\text{coul}} = ZeE$) with the viscous resistance ($F_{\text{vis}} = fv$), and it turns out to be $v = ZeE/3\pi\eta a$, where $Ze$ is the effective particle charge, $f$ is the friction factor, $a$ is the hydrodynamic diameter of the particle and $\eta$ is the viscosity of the liquid. Then the velocity per unit electric field is defined as the mobility of the particle

$$\mu_e = v/E = Ze/3\pi\eta a \tag{7}$$

and gives an indication of the nature of the charge on the colloidal particle. The hydrodynamic diameter of the particle is different from its actual diameter for the following reasons: the negatively charged particle accumulates positive ions around it due to simple electrostatic attraction and this process results in a complex structure that look something similar to what is shown in figure 5(b). When this complex particle moves in the liquid, the liquid near the surface of the particle also moves. The relative velocity decreases with the distance from the particle. The spherical area around the colloidal particle in which the ions firmly attach to the particle surface is known as the Stern layer [20]. When the particle moves in the liquid, the Stern layer is considered to move with it, while the outside layer (diffuse layer), which is less firmly associated with the particle, moves in a looser manner. As a result, the electric potential at the surface of the hydrodynamic layer is a complex issue; it is defined as the '$\zeta$ (zeta) potential'.

The magnitude of the $\zeta$ potential gives an indication of the stability of the colloidal system. The empirical threshold value of the $\zeta$ potential for particles in aqueous system is ±30 mV. Particles with a $\zeta$ potential more negative than −30 mV and more positive than +30 mV are normally considered to be stable [11, 12].

The $\zeta$ potential is frequently determined by first measuring the electrophoretic mobility. The electrophoretic mobility and

the $\zeta$ potential are related by the Henry equation [20] and are given by

$$\mu_e = 2\varepsilon\zeta f(\kappa r_s)/3\eta \quad (8)$$

in which $f(\kappa r_s)$ is the Henry function, $\kappa$ is the Debye screening parameter, $r_s$ is the geometric radius of the particle and other symbols have been described earlier.

In aqueous media and moderate electrolyte concentration, $f(\kappa r_s) = 1.5$, which is called the 'Smoluchowski approximation'. For small particles in media with a low dielectric constant $f(\kappa r_s) = 1$, and this is called the 'Hückel approximation'. Our analysis in this paper is done using the Hückel approximation, since we used hexane as the solvent in the electrophoretic mobility measurements.

As seen from figure 5(b), the 'charge' of the dots determined from the $\zeta$ potential measurements is the hydrodynamic charge and it is a convolution of the charge of the dots and the ionic charges surrounding the dots as they move in the hexane solution on their way to the electrodes. These complications in the charge of the dots and the broadening in the $\zeta$ potential measurements explain why quantitative analysis of the charge distribution of the maghemite NQDs in our EPD experiments is an extremely difficult task. Consequently, relative positive and negative areas in the $\zeta$ potential/mobility plots do not necessarily give the relative concentrations of the positively and negatively charged NQDs. Below we attempt to make some qualitative judgments on the charging nature of the maghemite dots based on the results of the $\zeta$ potential measurements as shown in figure 5(a).

It is clear that when the EPD films grow on both electrodes and the deposition stops, and the current becomes constant, the negative fractions (usually) approach zero. These observations suggest the following:

(1) In the hexane solution of the maghemite NQDs there are initially more positively charged 'ions' than negatively charged 'ions'. The word 'ion' here refers to a complex particle similar to that shown in figure 5(b).
(2) Counterions are present in the solution to maintain charge neutrality.
(3) An equal number of positively and negatively charged NQDs are deposited (and transfer their charges).
(4) EPD terminates because the negative ions are exhausted from the solution.
(5) The primary contribution to the current is from charge transfer from the charged dots at the electrodes. The counterions are not substantially involved because the film thicknesses do not reflect the relative proportions of the positively and negatively charged 'ions'.

The initial larger number of positively charged dots can be rationalized by some preferential removal of the capping ligands from the dot surface and the exposure of either the Fe or O atoms on the surface. In the absence of detailed theoretical studies done on these dots it may not be prudent to delve deeper into this issue.

Allowing the leftover dot solution after a typical EPD run to stand in a beaker for 2 days seems to increase the negative fraction and allow for continued EPD. This apparent change in the charge distribution probably originates from the loss of loosely bound ligand molecules or the movement of the ligands on the surfaces of the remaining dots. This could also be a result of thermal charging of the dots described in section 4.1.

Even though we are not able to describe the mechanism of the evolution of the $\zeta$ potential distribution quantitatively, the results do provide us with tremendous opportunity to fabricate NQD heterostructures. A typical scheme could be as follows: start with a pair of electrodes lithographically defined on a $SiO_2$ surface on a Si wafer; connect the electrodes with a DC power supply and submerge the wafer in a maghemite dot solution whose $\zeta$ potential distribution negative fraction has just reached zero. Maghemite dot film will be deposited only on the cathode and the anode will be bare. Now, remove the wafer from the maghemite dot solution and submerge it in a CdSe dot solution whose $\zeta$ potential distribution negative fraction has just reached zero [21], and this time connect the bare electrode to the negative DC potential and perform EPD. CdSe dot film will be deposited on this electrode. With careful control of the dot density, DC voltage and time of deposition, it should be possible to merge these two films, as shown schematically in figure 5(c). To the best of our knowledge this could be the first controlled magnetic/semiconducting NQD heterostructure. With careful choice of NQDs it should be possible to make many different kinds of NQD heterostructures using this scheme. This will help with devices requiring NQD band lineup engineering, like solar cells.

## 5. Conclusion

For NQDs to be electrophoretically deposited, they need to be charged and be able to transfer charges to and then stick to the electrode. Charging percentage measurements indicate that the maghemite dots are charged due to unpassivated surface sites, or more specifically surface facets. The removal of the ligands also makes them more 'sticky' by reducing the solubilization energy in the solvent and may help with charge transfer at the electrode surface. We argued in section 4.1 that since the charging is a thermodynamic process, there are equal numbers of positively and negatively charged maghemite dots, in general.

$\zeta$ potential/electrophoretic mobility measurement, however, forces us to review our conclusion based on thermodynamics alone. These measurements suggest that the concentrations of positively and negatively charged dots in the solution are not equal, so there are clearly counterions present in solution. Nonetheless, the formation of films of equal thickness on both electrodes suggests that the current observed during the deposition process arises mostly from the charged dots. The films can be grown only up to a certain maximum thickness because the limiting factor is the depletion of the negatively charged dots.

In general, $\zeta$ potential/electrophoretic mobility and the charging percentage measurements suggest that the removal of the ligands from the maghemite dot surface strongly influences the surface charges of the dots. Ligands play significant roles in influencing the physical properties of colloidal dots. Adjusting

the ligand chemistry will help us to obtain control over the charging of NQDs and will enable the optimization of the EPD process.

Finally, we suggested the feasibility of fabricating NQD heterostructures by exploiting the evolution of the $\zeta$ potential distribution of the dot solution.

## Acknowledgments

This work was supported by the MRSEC program of the National Science Foundation, award no. DMR-9809687, and an American University of Sharjah Faculty Research Grant FRG 2008-005.

## References

[1] Schwertmann U and Cornell R 2003 *The Iron Oxides: Structure, Properties, Reactions, Occurrences and Uses* (New York: Wiley–VCH)
[2] Murray C B, Kagan C R and Bawendi M G 1995 *Science* **270** 1335
[3] Collier C P, Saykally R J, Shiang J J, Henrichs S E and Heath J R 1997 *Science* **277** 1978
[4] Trau M, Saville D A and Aksay I A 1996 *Science* **272** 706
[5] Giersig M and Mulvaney P 1993 *Langmuir* **9** 3409
[6] Brust M, Walker M, Bethell D, Schiffrin D J and Whyman R 1994 *J. Chem. Soc. Chem. Commun.* **1994** 801
[7] Sun S, Murray C B, Weller D, Folks L and Moser A 2000 *Science* **287** 1989
[8] Hyeon T, Lee S S, Park J, Chung Y and Na H B 2001 *J. Am. Chem. Soc.* **123** 12798
[9] Islam M and Herman I 2003 *Appl. Phys. Lett.* **80** 3823
[10] Morrison I 1993 *Colloid Surf.* A **71** 1
[11] Zeta-Meter Inc. 1997 *Zeta Potential: a Complete Guide in 5 Minutes* http://www.zeta-meter.com/index.html
[12] *Colloids and Zeta Potential* Malvern Inc.
[13] Brus L 1983 *J. Chem. Phys.* **79** 5566
[14] Pokrant S and Whaley K 1999 *J. Chem. Phys.* **111** 6964
[15] Islam M 2008 *Nanotechnology* **19** 255708
[16] Islam M 2008 *Electrophoretic Deposition of Multifunctional Nanoparticle Films* 1st edn (Germany: VDM)
[17] Shim M and Guyot-Sionnest P 1999 *J. Chem. Phys.* **111** 6955
[18] Whittle M 1990 *J. Non-Newton. Fluid. Mech.* **37** 233
[19] Jackson J D 1968 *Classical Electrodynamics* 2nd edn (New York: Wiley)
[20] Hunter R 2001 *Foundations of Colloidal Science* 2nd edn (Oxford: Oxford University Press)
[21] Jia S, Banerjee S and Herman I 2008 *J. Phys. Chem.* C **112** 162